


Article

Dynamics of the Toxic Dinoflagellate *Alexandrium pacificum* in the Taiwan Strait and Its Linkages to Surrounding Populations

Minlu Liu ¹, Jing Zheng ¹, Bernd Krock ², Guangmao Ding ³, Lincoln MacKenzie ⁴, Kirsty F. Smith ⁴ and Haifeng Gu ^{1,5,*} 

¹ Third Institute of Oceanography, Ministry of Natural Resources, Xiamen 361005, China; liuminlu@tio.org.cn (M.L.); zhengjing@tio.org.cn (J.Z.)

² Alfred Wegener Institut-Helmholtz Zentrum für Polar-und Meeresforschung, Am Handelshafen 12, D-27570 Bremerhaven, Germany; bernd.krock@awi.de

³ Fishery Resources Monitoring Center of Fujian Province, Fuzhou 350003, China; haner1982@126.com

⁴ Cawthron Institute, 98 Halifax Street East, Private Bag 2, Nelson 7042, New Zealand; lincoln.mackenzie@cawthron.org.nz (L.M.); kirsty.smith@cawthron.org.nz (K.F.S.)

⁵ Key Laboratory of Marine Ecological Conservation and Restoration, Ministry of Natural Resources, Xiamen 361005, China

* Correspondence: guhaifeng@tio.org.cn; Tel.: +86-592-2195157

Abstract: The dinoflagellate *Alexandrium pacificum* can produce paralytic shellfish toxins and is mainly distributed in the Pacific. Blooms of *A. pacificum* have been frequently reported in offshore areas of the East China Sea, but not along the coast. To investigate the bloom dynamics of *A. pacificum* and their potential origins in the Taiwan Strait, we performed intensive sampling of both water and sediments from 2017 to 2020. Ellipsoidal cysts were identified as *A. pacificum* and enumerated based on microscopic observation. Their abundances were quite low but there was a maximum of 9.6 cysts cm⁻³ in the sediment near the Minjiang River estuary in May 2020, consistent with the high cell abundance in the water column in this area. Cells of *A. pacificum* were examined using a quantitative polymerase chain reaction, and they appeared to be persistent in the water column across the seasons. High densities of *A. pacificum* (10³ cells L⁻¹) were observed near the Jiulongjiang and Minjiang River estuary in early May 2020, where high nutrients (dissolved inorganic nitrogen and phosphate), and relatively low temperatures (20–21 °C) were also recorded. Strains isolated from the East and South China Sea exhibited the highest division rate (0.63 and 0.93 divisions d⁻¹) at 20 and 23 °C, respectively, but the strain from the Yellow Sea showed the highest division (0.40 divisions d⁻¹) at 17–23 °C. Strains from the East and South China Sea shared similar toxin profiles dominated by the *N*-sulfocarbamoyl toxins C1/2, but the strain from the Yellow Sea predominantly produced the carbamoyl toxins GTX1/4 and no C1/2. Our results suggest that both cyst germination and persistent cells in the water column might contribute to the bloom formation in the Taiwan Strait. Our results also indicate that the East and South China Sea populations are connected genetically through similar toxin formation but separated from the Yellow Sea population geographically.

Keywords: harmful algal blooms; cysts; growth; paralytic shellfish toxins



Citation: Liu, M.; Zheng, J.; Krock, B.; Ding, G.; MacKenzie, L.; Smith, K.F.; Gu, H. Dynamics of the Toxic Dinoflagellate *Alexandrium pacificum* in the Taiwan Strait and Its Linkages to Surrounding Populations. *Water* **2021**, *13*, 2681. <https://doi.org/10.3390/w13192681>

Academic Editor: Reynaldo Patiño

Received: 3 September 2021

Accepted: 25 September 2021

Published: 28 September 2021

Publisher's Note: MDPI stays neutral with regard to jurisdictional claims in published maps and institutional affiliations.



Copyright: © 2021 by the authors. Licensee MDPI, Basel, Switzerland. This article is an open access article distributed under the terms and conditions of the Creative Commons Attribution (CC BY) license (<https://creativecommons.org/licenses/by/4.0/>).

1. Introduction

Paralytic shellfish toxins (PST) are among the most devastating biotoxins; consumption of PST-contaminated bivalves may cause tingling and numbness, respiratory difficulty, and even death [1]. The dinoflagellate genus *Alexandrium* includes several PST-producing species, of which *Alexandrium catenella* Kofoid (previously *A. tamarensis* species complex Group I) and *A. pacificum* Litaker (previously *A. tamarensis* species complex group IV) are widely distributed. With fairly indistinguishable morphological characters, these two species and the other three species of the *A. tamarensis* species complex were redefined primarily based on molecular phylogeny, mating incompatibilities, and toxin production [2].

Alexandrium pacificum has been found in the Mediterranean (France, Italy, and Spain), North Pacific (China, Japan, Singapore, and South Korea), South Pacific (Australia and New Zealand), and the Southern Ocean [2]. *Alexandrium catenella* has a wider distribution area towards the cold-water regions, but *A. catenella* and *A. pacificum* often occurred in sympatry in North Pacific and Australia [2–5]. In China, *A. catenella* is mainly distributed in the Yellow Sea, while *A. pacificum* has been detected in the South and East China Sea and occasionally, in the Yellow Sea and Bohai Sea [6,7].

Like many other dinoflagellates, the life cycle of *A. pacificum* involves a cyst stage, which plays a vital role in population initiation, development, dispersal, and decline [4]. Cysts remain dominant in disadvantageous environmental conditions, e.g., nutrient limitation, low temperature, or darkness, and may germinate again when conditions become favorable, especially under certain disturbances, e.g., wind-induced re-suspension [8,9]. Furthermore, cysts greatly expand the dispersal range of dinoflagellate species because they can travel large distances via ballast water vectoring [10]. The distribution and abundance of *Alexandrium* cysts, and their contribution to bloom formation, has been frequently investigated [4,11–13]. The abundance of *A. pacificum* cysts is generally low in the East and South China Sea with a recorded maximum of ca. 24 cysts cm⁻³ or 30 cysts g⁻¹ of sediments at stations near the Changjiang River estuary [14,15]. A high abundance of *A. pacificum* cysts (503 cysts g⁻¹) was reported in Daya Bay, South China Sea [16]. The temporal and spatial mismatch between cyst germination and bloom outbreak implies that bloom formation is a complex process influenced by physical, chemical, and biological factors [4,17,18].

Alexandrium pacificum from different geographic areas show notable variation in ecophysiological traits. The highest abundance of *A. pacificum* cells have been observed in Kesenuma Bay, Japan, and in the East China Sea when the water temperature was ~20 °C [4,19]. In contrast, the abundance of *Alexandrium* spp. was high in Daya Bay, South China Sea, at the temperature of 22.8–30.0 °C [20]. However, these cells were likely a combination of *A. pacificum* and *A. minutum* [21]. Physiological adaptation of *A. pacificum* to local environments has also been supported by culture experiments. The optimum temperature for the growth of the strain ACT03 from Thau, France (Mediterranean Sea), was 20–27 °C [22], in contrast to 20–30 °C for an *A. pacificum* strain isolated from Jinhae-Masan Bay, Korea [23].

Alexandrium pacificum strains have low genetic divergence worldwide [2] but often show notable variation in toxin profiles. Most strains of *A. pacificum* from Japan, Australia, and the East and South China Sea have toxin profiles dominated by C1/2 [19,24–27]. However, the toxin profiles of *A. pacificum* strains from Korea and the Mediterranean are much more varied, dominated by C1/2, C3/4, or GTX1/4 in some strains [28–30]. The toxin profiles of *A. pacificum* and *A. catenella* isolates are distinctive and relatively consistent and thus may be related to their origins [26,31]. The toxin profiles of *A. pacificum* strains from the Yellow Sea of China have not yet been reported.

Alexandrium pacificum blooms have been frequently observed in the East China Sea [32], but the cyst densities here were quite low [15]. The Taiwan Strait connects to the East and South China Sea, although *A. pacificum* blooms are rarely reported in this area. However, they pose a potential threat to shellfish aquaculture along the Western coast of the Taiwan Strait where a production of as much as 4.3 million tons was recorded in 2016 [33]. Cysts of *A. pacificum* have been reported in several localities in the Taiwan Strait at low abundance [13], but intensive sampling has not yet been performed. This study aims to understand (1) the bloom mechanism of *A. pacificum* in the Taiwan Strait and (2) the relationship of the *A. pacificum* population in the Taiwan Strait to those in surrounding waters. We examined the seasonal dynamics of *A. pacificum* cysts and cells in the Taiwan Strait. The toxin profiles and growth rate of strains from the Taiwan Strait, South China Sea, Yellow Sea of China, and New Zealand are also reported.

2. Materials and Methods

2.1. Sample Collection and Treatment

Water and/or sediment samples were collected from December 2017 to December 2020 in the Taiwan Strait, Yellow Sea, South China Sea, and the Marlborough Sounds, New Zealand (Figure 1A,B, Table 1, Supplementary Table S1). In addition, water and/or sediment samples were collected monthly at three stations in Xiamen Bay from December 2017 to January 2020 and seasonally at 17 stations in Dongshan Bay from May 2019 to December 2020 (Figure 1C,D, Supplementary Tables S2 and S3). Two liters of water samples at 3 and 10 m depth were collected and prefiltered through a 200 μm mesh, subsequently filtered onto 5 μm pore-size polycarbonate filters (Millipore, Eschborn, Germany), and stored at $-20\text{ }^{\circ}\text{C}$ for DNA extraction. The concentration of chlorophyll *a* (Chl *a*), water temperature, dissolved oxygen (DO), turbidity, and salinity were measured using a YSI EXO Multi-Parameter Water Quality Sonde (Yellow Springs Instrument Company, Yellow Springs, OH, USA).

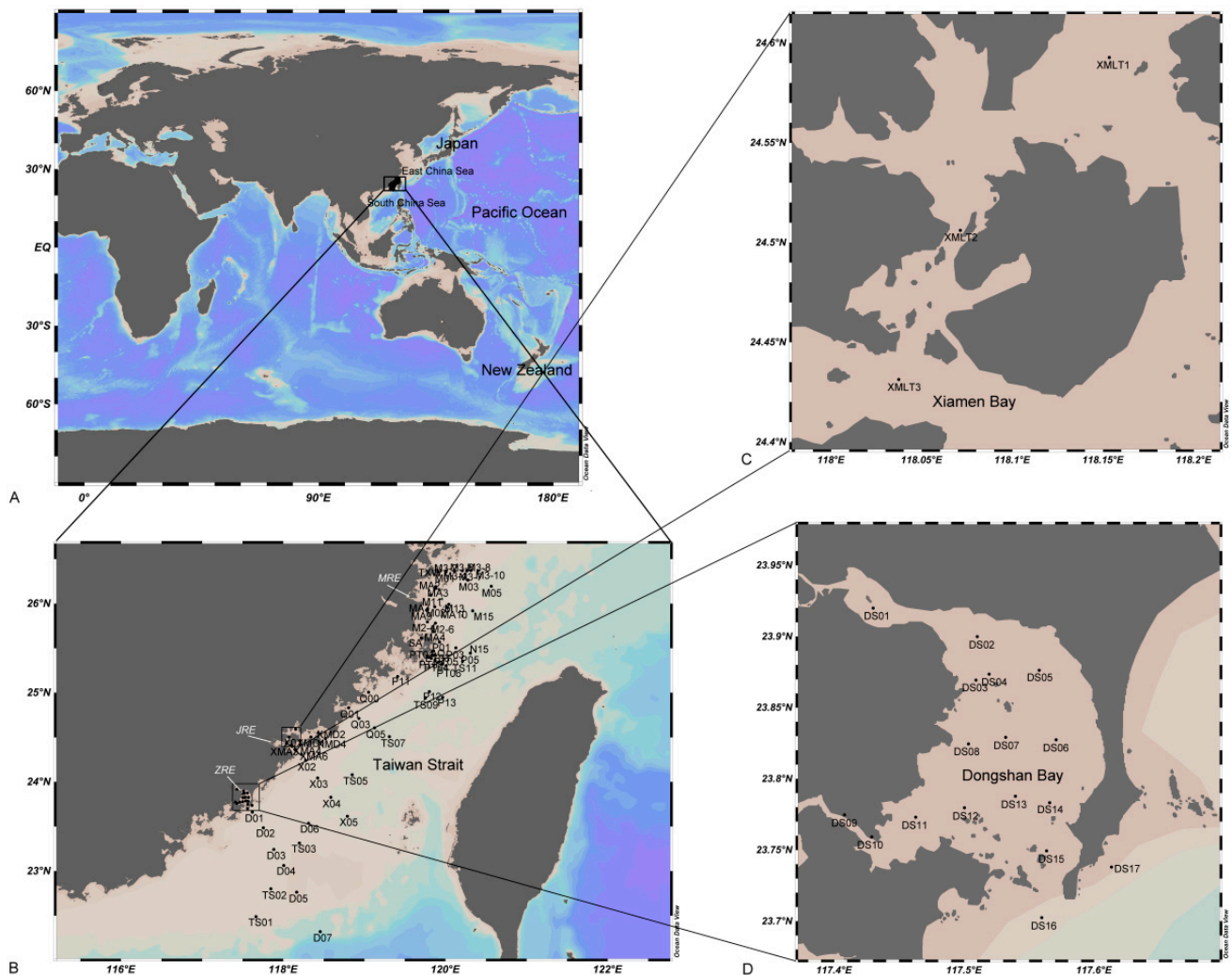


Figure 1. Sampling area and locations in the Taiwan Strait. (A) A world map showing the location of sampling areas. (B) Overview of stations (MRE: Minjiang River estuary, JRE: Jiulongjiang River estuary, ZRE: Zhangjiang River estuary). (C) Detailed view of the stations in Xiamen Bay. (D) Detailed view of the stations in Dongshan Bay.

Table 1. Information of strains examined in this study, including location, latitude, longitude, collection time, origin, toxin, and growth. NA: not available.

Strains	Location	Latitude	Longitude	Collection Time	Origin	Toxin	Growth Experiment
TIO855	Yantai, Yellow Sea	37°29.28' N	121°37.24' E	3 September 2016	Cell	Present	Yes
TIO1201	Qingdao, Yellow Sea	36°0.15' N	120°21.27' E	29 September 2017	Cyst	None	No
TIO1204	Taiwan Strait	25°57.90' N	119°52.10' E	16 November 2018	Cyst	Present	No
TIO1205	Taiwan Strait	25°57.90' N	119°52.10' E	16 November 2018	Cyst	NA	No
TIO1208	Taiwan Strait	25°57.90' N	119°52.10' E	16 November 2018	Cyst	NA	No
TIO987	Pingtang, Taiwan Strait	25°38.04' N	119°48.97' E	16 April 2020	Cell	Present	No
TIO989	Pingtang, Taiwan Strait	25°38.04' N	119°48.97' E	16 April 2020	Cell	Present	No
ATDH46	East China Sea	27°35.24' N	122°7.65' E	6 August 2009	Cyst	NA	Yes
TIO866	Beihai, South China Sea	21°0.64' N	109°6.05' E	11 April 2017	Cyst	Present	Yes
TIO1210	New Zealand	41°16.04' S	174°12.14' E	8 February 2018	Cyst	Present	No

Sediment samples were collected from a wide geographic area at random using a core sampler or box sampler, and only surface sediments (0–2 cm) were sliced off. About 2.5 cm³ of surface sediment samples were processed for cysts enumeration. Cysts were extracted using a sodium polytungstate density gradient with a density of 1.4 g cm⁻³ as detailed in Bolch [34] for direct cyst counting with an inverted Eclipse TS100 (Nikon, Tokyo, Japan) microscope. Cysts from the sediment or cells from the water sample were individually isolated with a micropipette using the above microscope to 96-well plates filled with 300 µL of f/2-Si medium [35] and incubated at 20 °C, 90 µmol photons m⁻² s⁻¹ under a 12: 12 h light: dark cycle (hereafter called standard conditions) for the establishment of nine strains (Table 1). Nearly all isolated cysts germinated within a week and gave rise to a culture. Cultures were maintained in 100 mL Erlenmeyer flasks under the standard conditions.

The 0.22 µm filtered seawater (100 mL) was stored at –20 °C for the measurements of nutrient concentration. The examination of nutrients was performed using a QuAAtro (Seal Analytical, Norderstedt, Germany) as previously reported [36]. Total dissolved inorganic nitrogen (DIN) was calculated based on the sum of ammonium, nitrate, and nitrite concentrations.

2.2. PCR Amplifications and Sequencing

The molecular sequences of nine strains of *A. pacificum* were examined (Table 1). Single cells were isolated from all nine strains and washed several times with sterile distilled water and used for templates. PCR amplifications were carried out using 1 × PCR buffer, 50 µM dNTP mixture, 0.2 µM of each primer, and 1 U of ExTaq DNA Polymerase (Takara, Tokyo, Japan) in 50 µL reactions. The LSU rRNA gene (D1–D6) was amplified using the primers D1R/28–1483R and following detailed procedures as previously reported [36]. Nine new LSU rRNA gene sequences have been deposited in GenBank (accession numbers OK178853 to OK178861).

2.3. Sequence Alignment and Phylogenetic Analysis

Newly obtained LSU rRNA (ca. 1300 bp) gene sequences were aligned with sequences of *Alexandrium* available in GenBank. Sequences were aligned using the MAFFT v7.110 [37] online program (<http://mafft.cbrc.jp/alignment/server/> (accessed on 3 Aug 2021)) with default settings. Alignments were manually checked with BioEdit v7.0.5 [38]. The final alignment consisted of 1233 base pairs including introduced gaps. The program jModelTest [39] was used to select the best model of molecular evolution with Akaike Information Criterion for Bayesian inference (BI). MrBayes 3.2 was used to perform Bayesian inference [40] with the substitution model (GTR+G) chosen by jModelTest. Four Markov chain Monte Carlo (MCMC) chains ran for 2,000,000 generations, sampling every 1000 generations. The first 10% of burn-in trees were discarded. A majority rule consensus tree was created to examine the posterior probabilities (BPP) of each clade. Maximum likelihood

(ML) analyses were conducted using RaxML v7.2.6 [41] on the T-REX web server [42] with the model GTR+G. Bootstrap support (BS) was evaluated with 1000 replicates.

2.4. Extraction of DNA

Total genomic DNA (gDNA) of water samples were extracted using the Nucleospin soil kit (Macherey & Nagel, Düren, Germany) following the manufacturer's instructions. DNA concentrations were analyzed using NanoDrop One Microvolume UV-Vis Spectrophotometer (ThermoFisher Scientific, Wilmington, DE, USA). DNA extraction efficiency was assessed by adding an exogenous plasmid pGEM-3Z (Promega, Tokyo, Japan) to a portion of the sample with target cells before (Sample 1) and after (Sample 2) DNA extraction, and dividing the copy number of pGEM-3Z computed from calibration curves of Samples 1 and 2 [43].

2.5. Quantitative PCR (qPCR)

Quantitative PCR was performed using the *A. pacificum* specific real-time PCR assay designed by Gao et al. [7] on a QuantStudio 1 real-time PCR detection system (Applied Biosystems, Foster City, CA, USA). The primers (AtIV-F and AtIV-R) and probe (AtIV-P) targeting the LSU rRNA gene [7] were synthesized and purified using HPLC (high performance liquid chromatography) (Sangon Biotechnology, Shanghai, China). The specificity of the primers and probe has been tested in a previous study using a BLAST search and hybrid experiment [7]. The optimised assays consisted of a 20 μ L reaction containing 10 μ L of 2 \times TaqMan Fast Advanced Master Mix (ThermoFisher Scientific, Wilmington, DE, USA), 900 nM of forward and reverse primers, 200 nM of fluorescent probe, and 2 μ L of DNA template. Cycling conditions were 50 $^{\circ}$ C for 2 min, 95 $^{\circ}$ C for 2 min, and 45 cycles of 95 $^{\circ}$ C for 15 s and 60 $^{\circ}$ C for 45 s.

The sensitivity of the assay was assessed with gDNA extracted from 1, 3, 5, and 10 cells. Calibration curves were constructed using serial dilutions of a known concentration of both synthetic gene fragment and cells [44]. A fragment of the LSU rRNA of *A. pacificum* flanked by both forward and reversed primers, with an extra ten base pair (bp) long at both ends, was synthesized (Sangon Biotechnology, Shanghai, China). A linear regression was performed onto the calibration curve to determine the R^2 value and slope. Amplification efficiency (AE) was calculated ($AE = [10(-1/\text{slope}) - 1] \times 100\%$). The copy numbers of LSU rRNA gene per cell of *A. pacificum* were determined from samples with known cell numbers based on the gene fragment calibration curve. Once the mean copy number of LSU rRNA gene per cell were confirmed, subsequent samples were examined by qPCR based on synthetic gene fragment as it was more stable and easy to preserve. All qPCR reactions were performed in triplicate and both negative control (no template control, NTC) and positive control (known concentration of synthetic gene fragment) were included.

To evaluate the qPCR assay performance in the field and to account for potential PCR inhibition effects of a natural seawater matrix, living cells of *A. pacificum* with known numbers were spiked into a natural seawater sample collected in Xiamen Bay. The absence of *A. pacificum* in the natural seawater was confirmed by light microscopy and qPCR. 10^5 , 10^4 , 10^3 , and 10^2 cells of *A. pacificum* were spiked into 50 mL of the natural seawater matrix in triplicates. Negative controls were also prepared using natural seawater without adding *A. pacificum* cells. The spiked seawater sample was subsequently filtered through 5 μ m filters, as described for the field samples, and then stored at -20° C until further processing. DNA of the spiked samples was extracted, subsequent qPCRs with gene fragment calibration curves were performed, and the *A. pacificum* cell number was calculated as described above.

2.6. Growth Experiment

Strains TIO855 (from the Yellow Sea), ATDH46 (from the East China Sea, as originally reported in Zou et al. [45]), and TIO866 (from the South China Sea) representing tropical, subtropical, and temperate populations were subjected to growth experiments. ATDH46

was chosen because strains from the Taiwan Strait did not grow well. Experiments on growth response to various temperatures (8, 11, 14, 17, 20, 23, 26, and 29 °C) were conducted in triplicate with 50 mL glass bottles containing 30 mL f/2-Si medium and an initial cell density of ~ 1000 cells mL⁻¹. Cultures were acclimated for 15 days to neighboring temperatures successively, at a step less than 3 °C at a time. The light: dark cycle was set as 12:12 h in all experiments. Subsamples of 0.05 mL were removed from the culture every two days and fixed in Lugol's solution. Each subsample was then transferred to a Sedgwick–Rafter chamber, and at least 200 cells per sample were counted. The growth rates in the exponential growth phase were calculated as described previously [46].

2.7. Analysis of Paralytic Shellfish Toxins

Approximately 70,000 cells of strains TIO1201 and TIO855 from Yellow Sea, strains TIO1204, TIO987, and TIO989 from East China Sea, strain TIO866 from South China Sea, and strain TIO1210 from New Zealand were collected in the exponential growth phase by a Universal 320 R centrifuge (Hettich-Zentrifugen, Tuttlingen, Germany) at $2500\times g$ for 10 min at 4 °C. Algal pellets were transferred to 2 mL microcentrifuge tubes and stored at -20 °C until analysis.

Cell pellets were resuspended in 500 μ L 0.03 M acetic and homogenized with 0.9 g of lysing matrix D by reciprocal shaking at 6.5 m s⁻¹ for 45 s in a Bio101 FastPrep instrument (Thermo Savant, Illkirch, France). Samples were then centrifuged at $16,100\times g$ for 15 min at 4 °C. The supernatants were transferred to spin-filters of 0.45 μ m pore-size (Millipore Ultrafree, Eschborn, Germany) and centrifuged for 30 s at $800\times g$, and then transferred to autosampler vials until measurement by LC-MS/MS.

Measurements were performed in the selected reaction monitoring (SRM) mode on a Xevo TQ-XS triple quadrupole mass spectrometer equipped with a Z-Spray source (Waters, Eschborn, Germany). Chromatographic separation was achieved on an Acquity UPLC Glycan BEH Amide column (130 Å, 150 mm \times 2.1 mm, 1.7 μ m, Waters, Eschborn, Germany) equipped with an in-line 0.2 μ m Acquity filter and thermostated at 60 °C with an isocratic elution to 5 min with 98% eluent B followed by a linear gradient of 2.5 min to 50% B and 1.5 min isocratic elution. The flow rate was 0.4 mL min⁻¹, and the injection volume was 2 μ L. Mobile A comprised water with 0.15 % formic acid and 0.6 % ammonia. Mobile B comprised water/acetonitrile (3:7, *v/v*) with 0.1% formic acid. PSTs were quantified by external calibration with standard mix solutions of four concentration levels consisting of the following PSTs: STX, NEO, GTX2/3, GTX1/4, dcSTX, dcNEO, dcGTX2/3, dcGTX1/4, B1(GTX5), B2(GTX6), C1/2, and C3/4 purchased from the Certified Reference Materials Program (CRMP) of the Institute for Marine Biosciences, National Research Council (Halifax, NS, Canada).

2.8. Statistical Analysis

The presented maps in this study were generated using the program “Ocean Data View” (ODV), version 5.1.0 [47].

3. Results

3.1. Molecular Identification of *A. pacificum*

Nine strains of *A. pacificum* from the Taiwan Strait, South China Sea, Yellow Sea, and New Zealand (Table 1) shared nearly identical LSU rRNA gene sequences and differed from each other only in one position. They grouped together with those strains from South Korea, Australia, and the Mediterranean Sea (Figure 2).

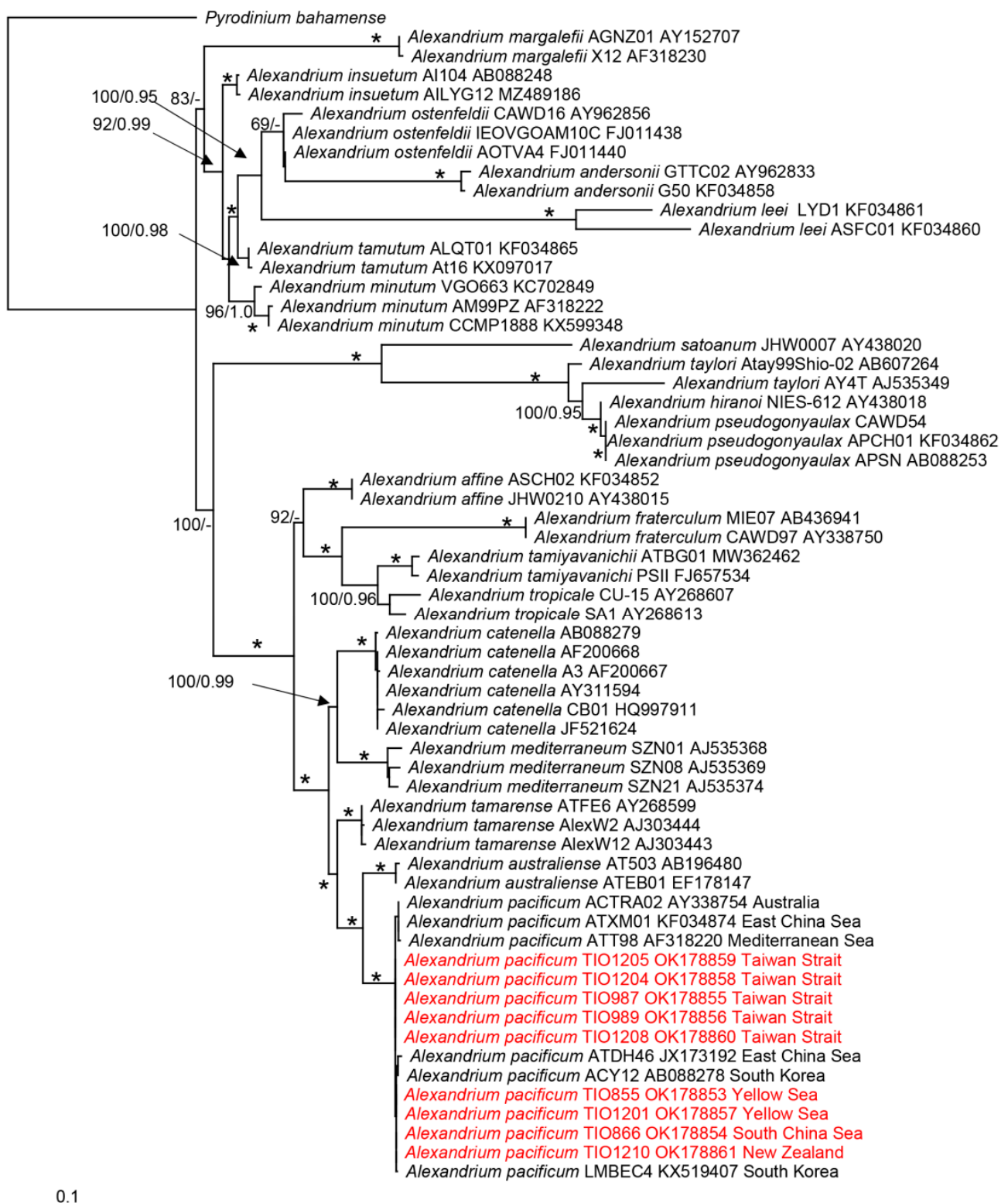


Figure 2. Molecular phylogeny of *Alexandrium pacificum* inferred from partial LSU rRNA (D1–D6) sequences using maximum likelihood (ML). New sequences are indicated in red. Branch lengths are drawn to scale, with the scale bar indicating the number of nucleotide substitutions per site. Numbers on branches are statistical support values to clusters on the right of them (**left**: ML bootstrap support (BS) values; **right**: Bayesian posterior probabilities (BPP)). BS values > 50% and BPP above 0.9 are shown. * indicates maximal support (BS = 100% and BPP = 1.00).

3.2. Assessment of the DNA Extraction Procedure

The concentration of the DNA extracts in this study ranged from 57 to 266 ng μL^{-1} . The qPCR results of the pGEM-3Z exogenous control in samples before and after gDNA extractions showed that Cq was delayed by approximately one unit, and the average correction factor (extraction efficiency) was 0.53 (Supplementary Table S4). Since a consistent gDNA extraction procedure was applied for all samples in the study, quantification could be performed without considering the correction factor.

3.3. Assessment of the qPCR Assay

The negative control in each qPCR run showed no signal of amplification. The gene-based calibration curve had a linear detection ranging over seven orders of magnitude ($R^2 = 0.9996$, AE = 96.8%; Supplementary Figure S1). The qPCR assay could detect a minimum of 10^4 gene copies. The cell-based calibration curve was also linear over seven orders of magnitude ($R^2 = 0.9984$; AE = 99.5%; Supplementary Figure S2).

Evaluation of the assay sensitivity showed that our qPCR assay was able to detect a consistent Cq from one (Cq = 27.44 ± 0.39), three (Cq = 26.03 ± 0.48), five (Cq = 25.27 ± 0.22), and 10 (Cq = 24.24 ± 0.27) target cells, respectively. Therefore, the minimum number of cells for a reliable quantification was one cell per reaction. The average LSU copy numbers per cell of *A. pacificum* in this study was $168,550 \pm 18,780$ (slope \pm SD) ($R^2 = 0.9992$, $p < 0.0001$; Supplementary Figure S3).

The recovery rate for different cell numbers of *A. pacificum* by spike experiments ranged from 87% to 121%. Cell number estimation using the gene-based calibration curve showed a positive correlation with the number of spiked cells determined microscopically ($R^2 = 0.9983$, $p < 0.0001$; Supplementary Figure S4).

3.4. Cyst Dynamics in the Taiwan Strait

Cyst abundances of *A. pacificum* were very low in the Taiwan Strait. Cysts were detected at two out of 10 stations in November 2018, with an abundance of 0.8 cysts cm^{-3} (Figure 3A). No cysts were detected in May 2019 (Figure 3B). Cysts were found in three out of eight stations in July 2019, with abundances that ranged from 0.8 to 3.2 cysts cm^{-3} (Figure 3C). In May 2020, cysts were found at seven out of 30 stations, with abundances ranging from 0.4 to 9.6 cysts cm^{-3} ; the highest density was recorded at the station near the Minjiang River estuary (Figure 3D). In August 2020, cysts were detected at two out of 24 stations, with abundances of 0.4 and 0.8 cysts cm^{-3} (Figure 3E).

3.5. Cell Dynamics in the Taiwan Strait Using qPCR

Alexandrium pacificum cells were detected at four stations in November 2018, with the highest abundance of ~ 18 cells L^{-1} near Quanzhou (Figure 4A). Cells were detected at six stations in May 2019, with the highest abundance of ~ 99 cells L^{-1} near the Minjiang River estuary (Figure 4B). In July 2019, cells were found in only one station near Jiulongjiang River estuary with a density of 2 cells L^{-1} (Figure 4C). In October and November 2019, cells appeared at two stations out of the Zhangjiang and Minjiang River estuary, with an abundance of around 139 and 15 cells L^{-1} , respectively (Figure 4D).

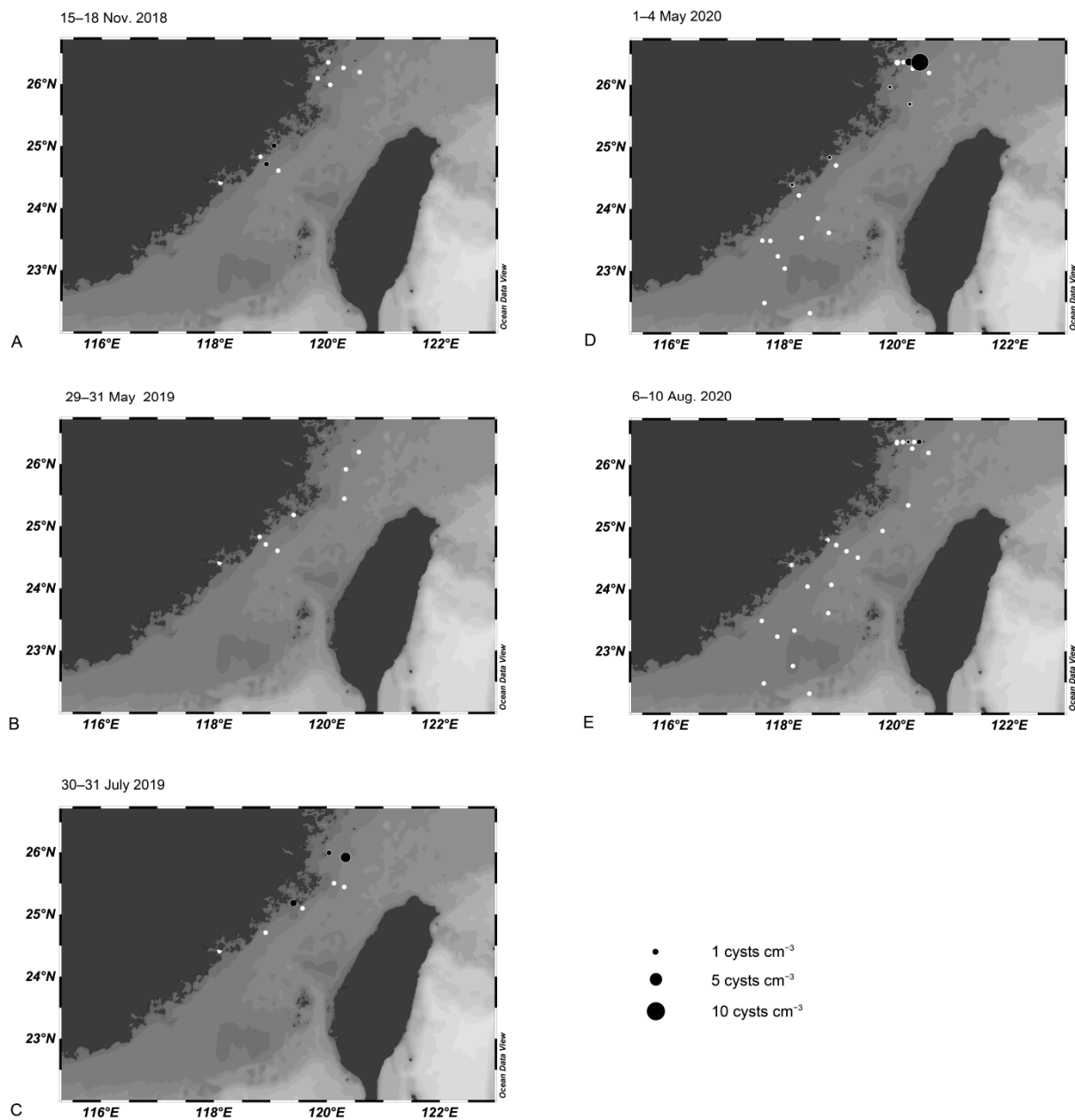


Figure 3. Cyst abundance (cysts cm⁻³) of *Alexandrium pacificum* in sediment samples from the Taiwan Strait in November 2018 (A), May 2019 (B), July 2019 (C), May 2020 (D), and August 2020 (E). White dots represent collection sites where no cysts were detected.

Between 1–4 May 2020, cells were detected at six out of 28 stations, ~1233 cells L⁻¹ at the station near Jiulongjiang River estuary, and ~841 cells L⁻¹ near the Minjiang River estuary (Figure 4E). On 12 May 2020, an abundance of ~4610 cells L⁻¹ was recorded near the Minjiang River estuary (Figure 4F). On 28 May 2020, ~452 cells L⁻¹ was recorded near Jiulongjiang River estuary (Figure 4G). Cells were present at 10 stations in August 2020 but the highest abundance was only ~22 cells L⁻¹ at the station near the Zhangjiang River estuary (Figure 4H).

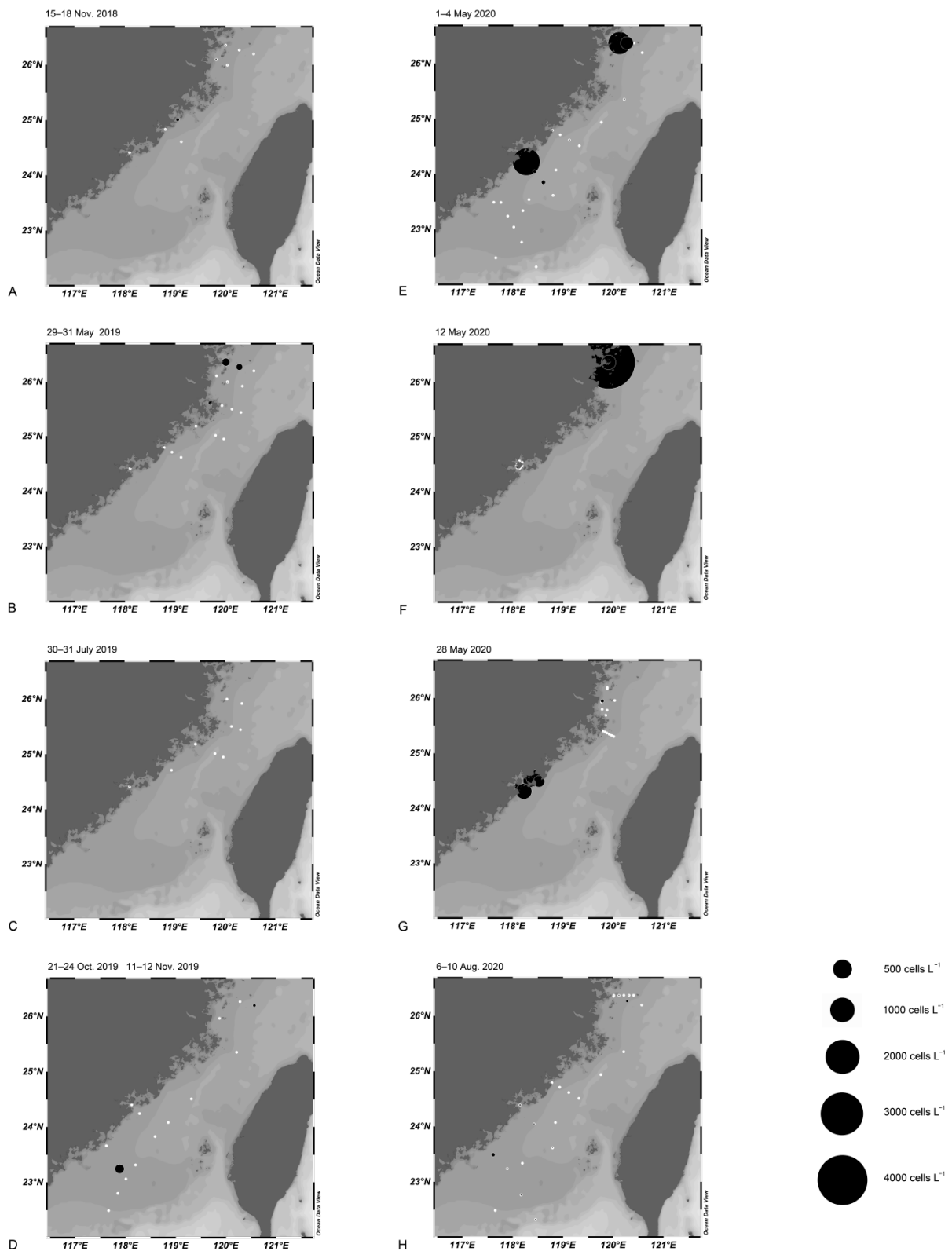


Figure 4. Cell abundance (cells L⁻¹) of *Alexandrium pacificum* determined by qPCR in water samples from the Taiwan Strait in November 2018 (A), May 2019 (B), July 2019 (C), October and November 2019 (D), May 2020 (E–G), and August 2020 (H). White dots represent collection sites where no cells were detected.

3.6. Cell Dynamics in Dongshan Bay and Xiamen Bay Using qPCR

Cells of *A. pacificum* were detected at three stations of Dongshan Bay in May 2019, with the highest abundance of ~ 10 cells L^{-1} at the station inside the bay mouth (Figure 5A). No cells were found in August 2019 (Figure 5B). Cells were detected in two stations in December 2019; the highest abundance was ~ 3 cells L^{-1} outside the bay mouth (Figure 5C). In July 2020, cells were found at three stations, with the highest abundance of ~ 240 cells L^{-1} inside the bay mouth (Figure 5D). No cells were found in August and December of 2020 (Figure 5E,F).

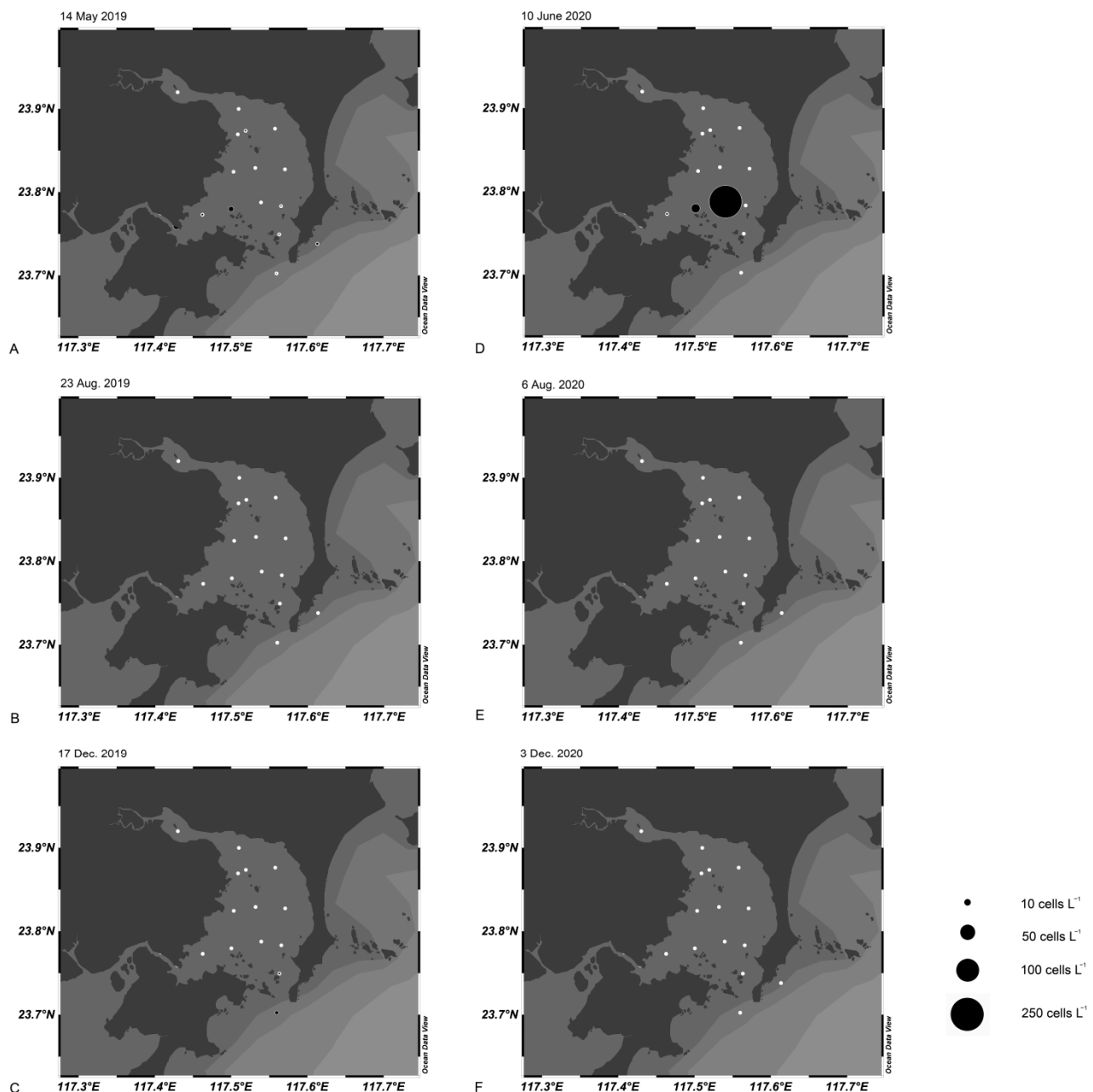


Figure 5. Cell abundance (cells L^{-1}) of *Alexandrium pacificum* determined by qPCR in water samples from Dongshan Bay in May 2019 (A), August 2019 (B), December 2019 (C), June 2020 (D), August 2020 (E), and December 2020 (F). White dots represent collection sites where no cells were detected.

Cells were detected in Xiamen Bay from December 2017 to January 2020, with a cell abundance of approximately 5.6 cells L^{-1} in December 2017; 19.6, 6.1, and 14.5 cells L^{-1}

in February, March and April 2018; and 4.9 and 4.2 cells L⁻¹ in March and April 2019, respectively (Figure 6A), when the water temperature was between 15.6 and 24.0 °C (Figure 6B).

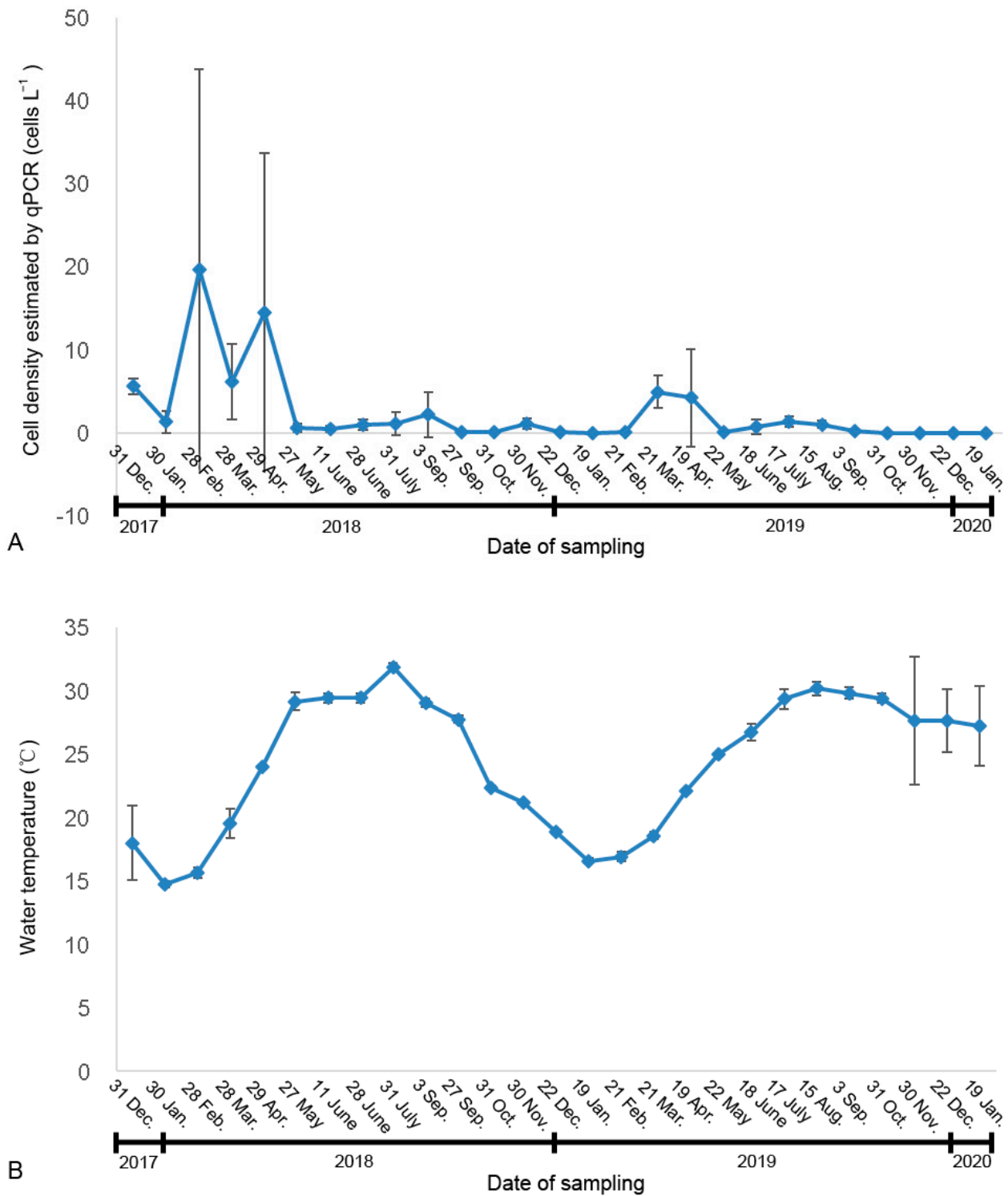


Figure 6. Average cell abundance (cells L⁻¹) of *Alexandrium pacificum* in water samples from the three stations in Xiamen Bay from December 2017 to January 2020. (A) Average cell abundance examined by qPCR and (B) average water temperature of the three stations in Xiamen Bay.

3.7. Growth Experiments

Strain TIO855 isolated from the Yellow Sea showed growth at temperatures between 11 and 26 °C. The highest division rate was ~ 0.40 divisions d^{-1} at 17–23 °C, which then decreased slowly towards higher and lower temperatures. Division rates were similar at temperatures of 11, 14, and 26 °C (~ 0.30 – 0.31 divisions d^{-1}). Almost no divisions occurred at 8 and 29 °C (Figure 7A).

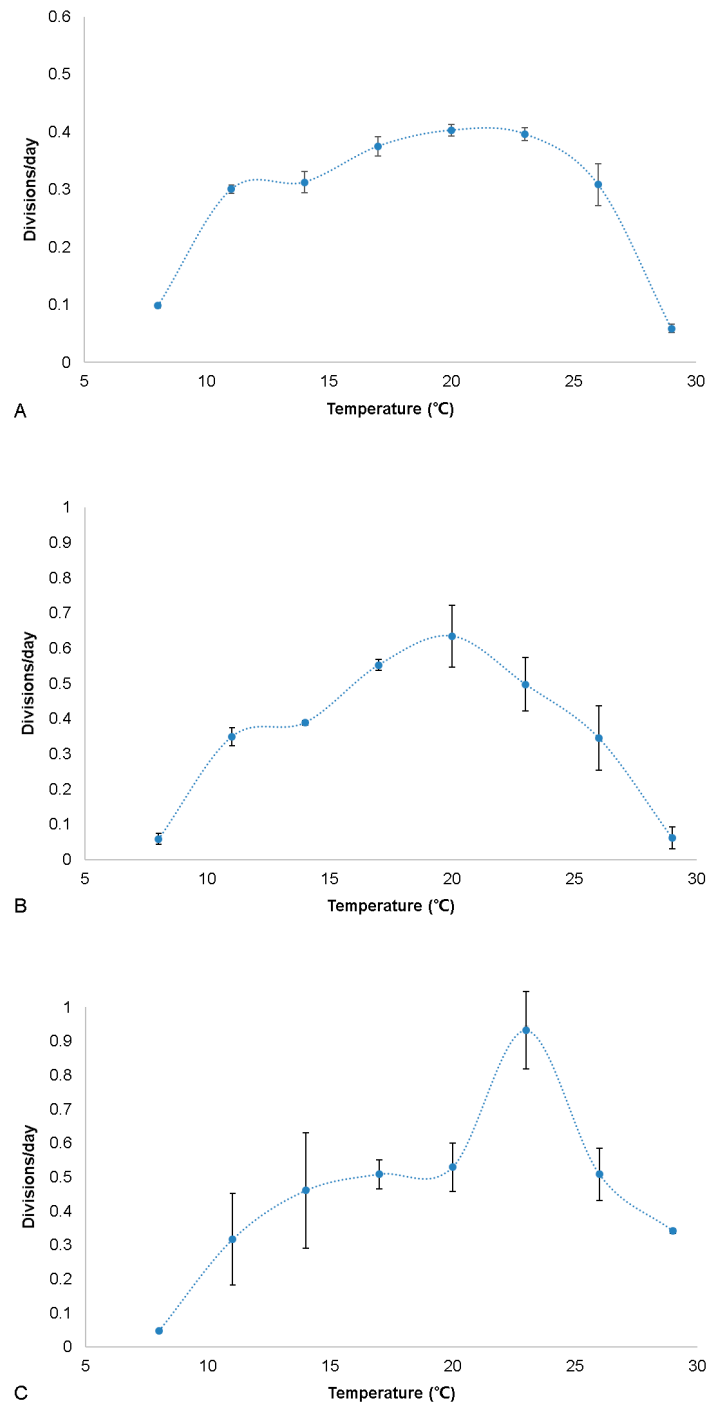


Figure 7. Growth responses of *Alexandrium pacificum* to various temperatures. (A) Strain TIO855 from the Yellow Sea, (B) strain ATDH46 from the East China Sea, and (C) strain TIO866 from the South China Sea. The values refer to mean divisions day^{-1} and the error bars refer to standard deviations.

Strain ATDH46 isolated from the East China Sea exhibited growth at temperatures between 11 and 26 °C. The highest division rate was 0.63 divisions d^{-1} at 20 °C and then dropped towards higher and lower temperatures. The division rates were 0.39, 0.55, and 0.50 divisions d^{-1} at 14, 17, and 23 °C, respectively. Division rates were similar at temperatures of 11 and 26 °C (~0.35 divisions d^{-1}). Almost no division occurred at 8 and 29 °C (Figure 7B).

Strain TIO866 isolated from the South China Sea exhibited growth at temperatures between 11 and 29 °C. The highest division rate was 0.93 divisions d^{-1} at 23 °C, which then decreased sharply towards higher and lower temperatures. The division rates were similar at temperatures of 17, 20 and 26 °C (around 0.5 divisions d^{-1}). Division rate was 0.32, 0.46, and 0.34 divisions d^{-1} at 11, 14, and 29 °C, respectively. Almost no division occurred at 8 °C (Figure 7C).

3.8. Toxin Profiles

All seven strains examined were able to produce PSTs except for strain TIO1201 from the Yellow Sea. Other strains did not grow well and were excluded from examination. *N*-sulfocarbamoyl toxins (C1/2 and B1) were produced by strains isolated from the East and South China Sea and the South Pacific Ocean; among them, C1/2 (0.13–0.76 $pg\ cell^{-1}$) were dominant, followed by B1 (0.02–0.12 $pg\ cell^{-1}$). In contrast, the carbamoyl toxins GTX1/4 (6.13 $pg\ cell^{-1}$) were dominant in strain TIO855 isolated from the Yellow Sea, followed by GTX2/3 (1.82 $pg\ cell^{-1}$) (Figure 8).

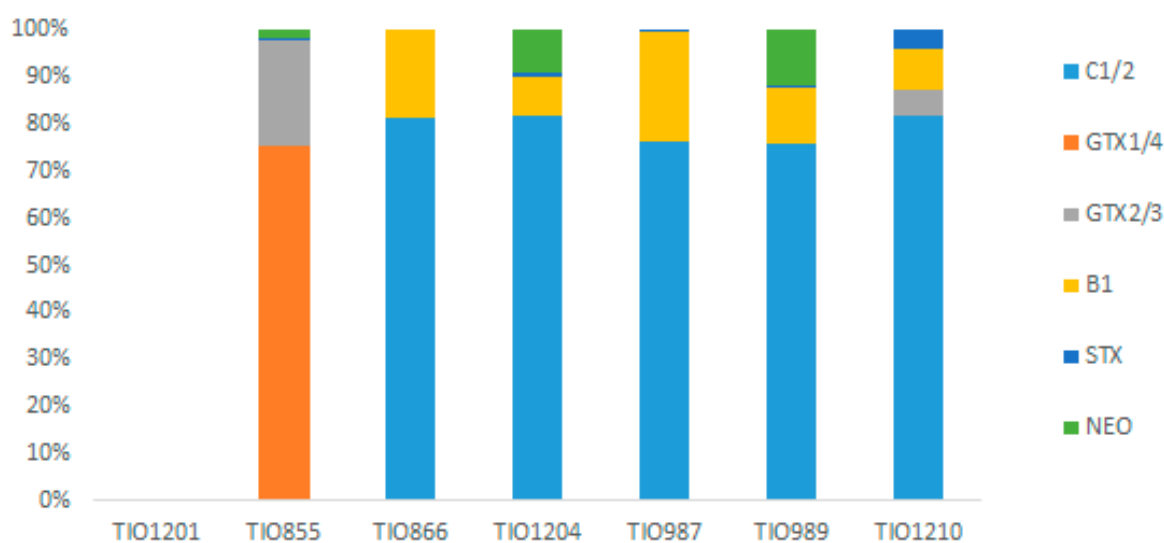


Figure 8. Histograms showing the relative PSP toxin composition (mol %) of *Alexandrium pacificum* strains. Strain TIO1201 did not produce detectable PSP toxin.

3.9. Environmental Parameters in the Taiwan Strait in May 2019 and 2020

The water temperatures ranged from 21.6 to 25.2 °C in 2019 (Figure 9A) and from 18.8 to 26.5 °C in 2020, with the lowest water temperature recorded near the Minjiang River estuary (Figure 9F). Salinity ranged from 27.4 to 34.6 in 2019 (Figure 9B) and from 27.8 to 35.6 in 2020, with the lowest salinity recorded near the Minjiang River estuary (Figure 9G). The maximum turbidity was 5.3 NTU near the Jiulongjiang River in 2020 (Figure 9C), compared to 10.4 NTU outside Quanzhou Bay in 2019 (Figure 9H). There were peaks of Chl *a* (12.6 $\mu g\ L^{-1}$) and ODO (10.2 $mg\ L^{-1}$) near the Minjiang River estuary in 2020 (Figure 9I,J) but not in 2019 (Figure 9D,E).

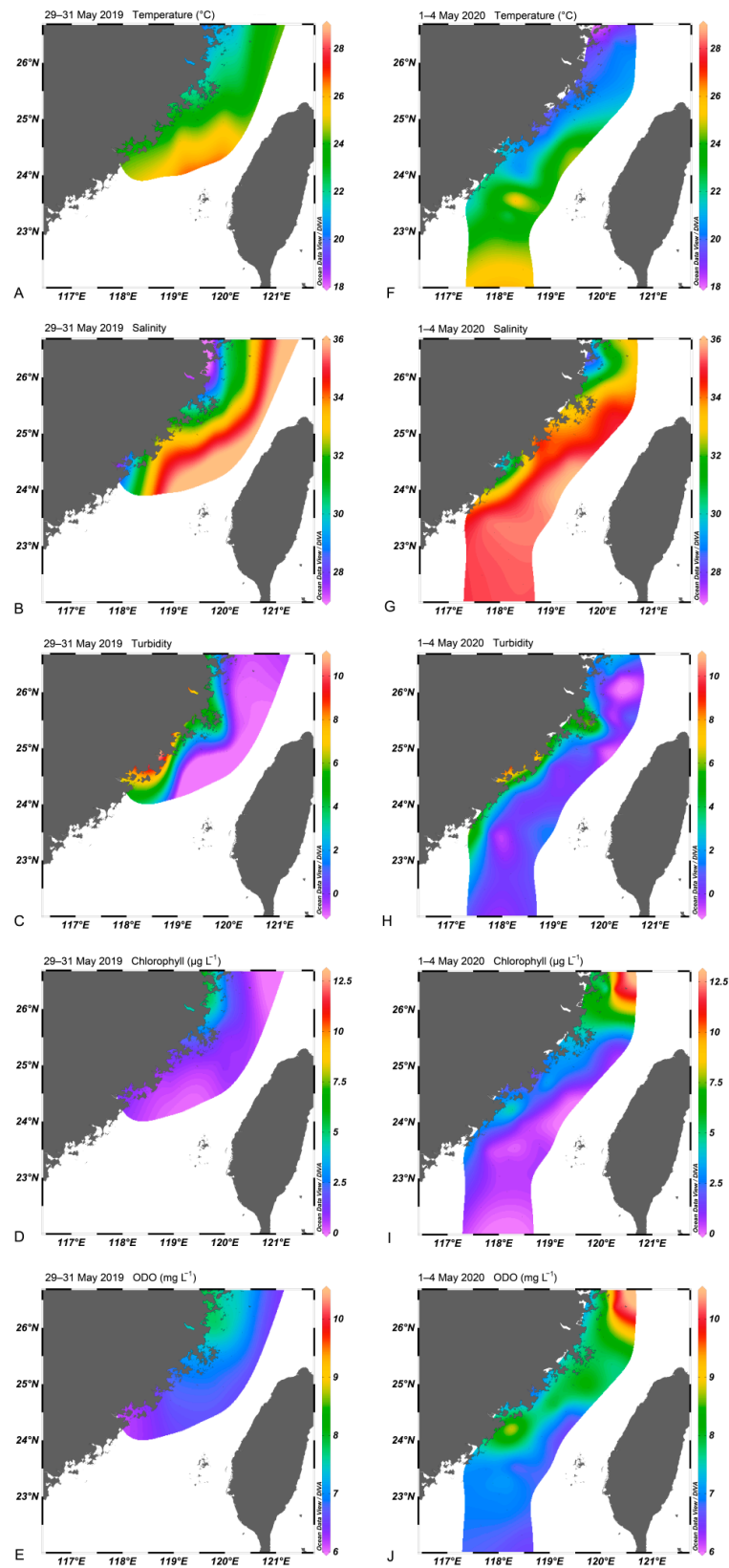


Figure 9. Water temperature ($^{\circ}\text{C}$) (A), salinity (B), turbidity (NTU) (C), chlorophyll ($\mu\text{g L}^{-1}$) (D), and dissolved oxygen (mg L^{-1}) (E) in the Taiwan Strait in May 2019. Water temperature ($^{\circ}\text{C}$) (F), salinity (G), turbidity (NTU) (H), chlorophyll ($\mu\text{g L}^{-1}$) (I), and dissolved oxygen (mg L^{-1}) (J) in the Taiwan Strait in May 2020.

3.10. Nutrient Concentrations in the Taiwan Strait in May 2020

Nutrient concentrations were quite high at the stations near the Minjiang River estuary and Jiulongjiang River estuary. The maximum concentration of PO_4^{3-} and DIN (NO_2^- , NO_3^- , and NH_4^+) was 1.017 and 18.722 $\mu\text{mol L}^{-1}$, respectively, near the Minjiang River estuary (Figure 10A,B).

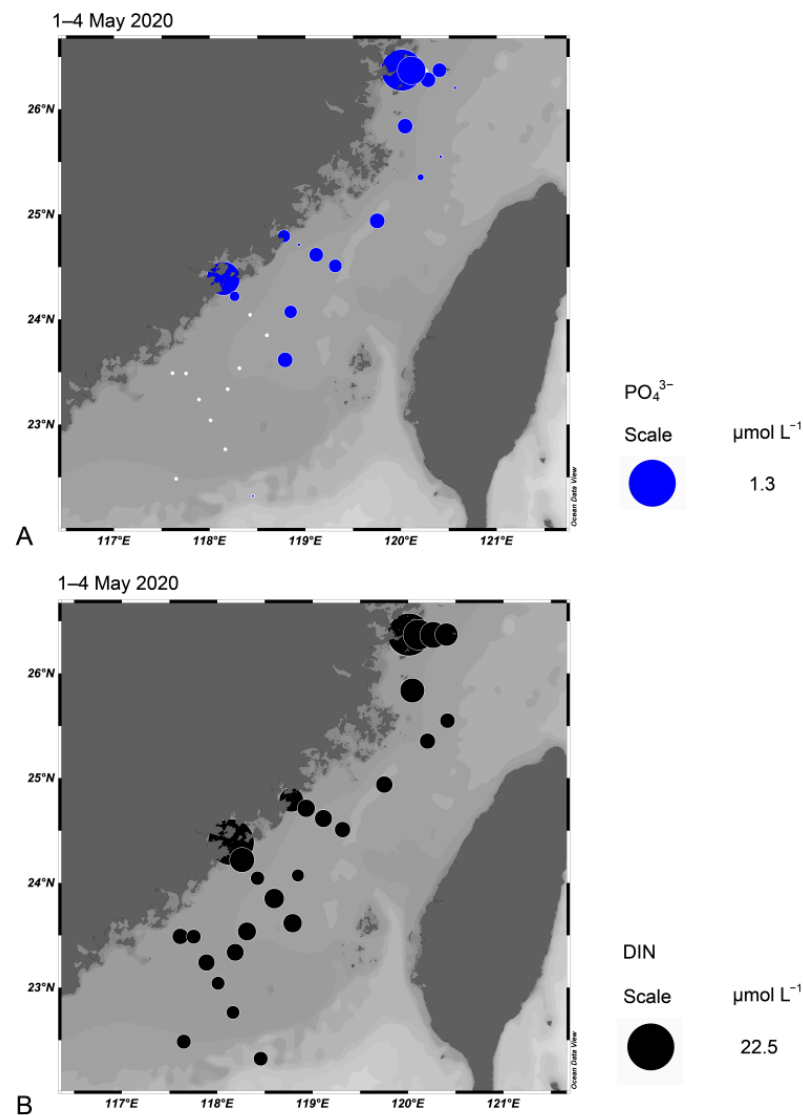


Figure 10. Concentration (μM) of (A) PO_4^{3-} and (B) DIN (NO_2^- , NO_3^- , and NH_4^+) in water samples collected in the Taiwan Strait in May 2020.

4. Discussion

4.1. Spatio-Temporal Distribution of *A. pacificum* Cells in the Taiwan Strait and Surrounding Waters

High densities of *A. pacificum* (10^3 – 10^6 cells L^{-1} , as *Alexandrium* sp.) were observed in the East China Sea from 2004 to 2007 [19,32]. However, these investigations were based on microscopic observations only; thus, the reported cell numbers may be overestimates since morphologically similar species, such as *Alexandrium affine*, are also present in this area [6]. To the best of our knowledge, this is the first attempt to quantify *A. pacificum* cells using a molecular approach focusing on the East China Sea.

A previous survey based on qPCR revealed a maximum *A. pacificum* abundance of 554 cells L^{-1} in the joint area between the Yellow Sea and East China Sea, but the abundance

was generally less than 20 cells L⁻¹ in the Yellow Sea and Bohai Sea [7]. This survey was carried out in May 2012, similar to our survey in the Taiwan Strait, in which *A. pacificum* abundance as high as 10³ cells L⁻¹ were recorded. Blooms of *A. pacificum* occurred in central Japan much later (from July to September) but the water temperature was almost the same (~20 °C) [4]. Blooms of *A. pacificum* have not yet been confirmed in northern China but an intensive bloom (10⁸ cells L⁻¹) of *Alexandrium tamarense* broke out in the Bohai Strait in September 2006, causing massive mortality of abalone [48]. The responsible species was likely to be *A. pacificum* as the water temperature was ~23 °C during the bloom [48], based on the fact that *A. catenella* prefers lower temperatures [4].

Unlike the blooms of *A. pacificum* recorded 100 km away from the Zhejiang coast of the East China Sea [32], high cell densities were observed near the Taiwan Strait coast. The average annual sediment load into East China Sea from the Changjiang River is 22.9 GT, but the Minjiang River discharges much less sediment (0.4 GT) to the Taiwan Strait [49]. This results in much higher turbidity along the coast of East China Sea (Zhejiang province) than that along the western Taiwan Strait coast (Fujian province) and may explain the spatial distinction of blooms between these two areas. It is worth noting that the western coast of Taiwan Strait is an important area for shellfish culture [33]; thus, routine monitoring of PSTs in shellfish is needed during the bloom season. In addition, our results suggest that intensive monitoring of *A. pacificum* cells using a molecular approach in early May will provide an early warning of potential blooms. In fact, monthly sampling in Xiamen Bay revealed a relatively high abundance of *A. pacificum* cells in early spring (Figure 6A).

Alexandrium catenella has been reported to prefer less saline and nutrient-rich waters provided by river runoff [50,51], which might also apply to *A. pacificum*. The maximum nutrient concentrations were recorded near the Minjiang and Jiulongjiang River estuary in early May 2020, where high abundances of *A. pacificum* cells (~1000 cells L⁻¹) were also recorded (Figure 4). The patchy distribution of *A. pacificum* cells supports the idea that a unique set of environmental and oceanographic forcing has determined the timing and extent of bloom development, as also demonstrated in *A. catenella* [52].

4.2. Possible Origins of *A. pacificum* Blooms in the Taiwan Strait

Both *A. catenella* and *A. pacificum* are able to produce ellipsoidal cysts that cannot be differentiated morphologically, but previous surveys have demonstrated that only *A. pacificum* is present in the East China Sea [6,15]. Therefore, we consider the ellipsoidal cysts in the Taiwan Strait are true *A. pacificum* and reveal that cyst densities were very low along the western coast of Taiwan Strait from 2018 to 2020. The findings of a maximum cyst density of *A. pacificum* (9.6 cysts cm⁻³) in the Taiwan Strait are consistent with previous investigations (maximum: 23.5 cysts cm⁻³ or 30 cysts g⁻¹ dry weight [DW]⁻¹) in the East China Sea [14,15], although blooms of *A. pacificum* have been frequently observed there [32]. The currents in the Taiwan Strait are often strong and can reach 0.45 m s⁻¹ [53], which is unfavorable for cyst accumulation. In addition, the dormancy of *A. pacificum* cysts is less than 2 weeks, after which they are ready to germinate under suitable environmental conditions [14], which is further disadvantageous for the formation of cyst banks. The cyst density of *A. pacificum* was extremely low in Xiamen Bay and Dongshan Bay (Gu, personal observation), but a high abundance in the other 11 bays in the Taiwan Strait cannot be excluded and will be the focus of future study. In fact, several patches with high cyst densities up to 440 cysts g DW⁻¹ were recorded in Thau Lagoon, although the average cyst density was less than 20 cysts g DW⁻¹ [17].

The formation of the initial population of *A. pacificum* by peak cyst germination is important for subsequent blooms 1–2 months later in Kesenuma Bay of central Japan [4]. The role of excystment in bloom initiation in the Taiwan Strait cannot be underestimated because cysts in the surface sediment at low abundances (2–25 cysts cm⁻³) can provide an inoculum of vegetative cells for bloom initiation [54]. Cyst abundance of *A. pacificum* was less than 10 cysts cm⁻³ in the Taiwan Strait but it apparently falls within this range. Alternatively, the persistent presence of cells in the water column, as many as 15–18 cells L⁻¹

in winter (Figure 3A,D), is also likely to lead to proliferation into high density blooms in spring when coincident with favorable physical, chemical, and biological factors, as observed in *A. catenella* [55].

4.3. Identifying Populations Based on Physiological Differentiation

The optimum water temperature of the cultured strains of *A. pacificum* from the East and South China Sea was 20 and 23 °C, respectively, similar to strains from Japan, Korea, Australia, and the Mediterranean Sea, showing optimum growth temperatures from 20 °C to 25 °C [4,22,23,27,56]. Strain TIO855 from the Yellow Sea showed lower division rates (0.06 divisions d⁻¹) at 29 °C compared to the 0.34 divisions d⁻¹ of the South China Sea strain TIO866, suggesting that geographically separated populations are adapted to local environments.

In addition to the differentiation in division rates, the toxin profiles of *A. pacificum* strains from different areas, or even from the same region, also varied significantly [18,45]. However, the dominance of C1/2 toxins appeared to be characteristics of *A. pacificum* strains isolated from the East China Sea [45]. These strains were established exclusively from resting cysts but C1/2 were also the dominant toxins in the bloom samples of *A. pacificum* in the East China Sea [32]. Three new strains of *A. pacificum* from water column and sediments in the Taiwan Strait also produced predominantly C1/2, thus supporting the notion that they belong to the same population as a result of rapid transition between cyst and cell stages. In terms of toxin profiles, *A. pacificum* strains from the East China Sea were similar to Japanese strains as they both produced predominantly C1/2 but the latter also produced predominantly GTX1/4 or B1 [57]. These results suggest that gene flow between these two populations is infrequent, although limited gene flow may have occurred based on microsatellite data [58].

To the best of our knowledge, this is the first report of the toxin profiles of *A. pacificum* from northern China, although this species is known to be present in the Bohai Sea and Yellow Sea of China [7,59]. One of these strains produced predominantly GTX1/4 but lacked C toxins. These types of toxin profiles are unusual and not found in strains from elsewhere (Supplementary Table S5). The saxitoxin (STX) biosynthesis pathway includes a group of genes, which form a gene cluster in cyanobacteria *Cylindrospermopsis raciborskii* [60]. Comparative transcriptomics of toxin synthesis genes revealed that most of the key genes for STX synthesis are present in *A. pacificum* [61]. The unusual toxin profile of *A. pacificum* from Yellow Sea likely resulted from the failure to produce N-sulfocarbamoyl toxins due to the lack of sulfotransferases, which is related with the production of N-sulfocarbamoyl toxins by the sulfoconjugation process [62]. GTX1/4 toxins are more potent than C1/2; thus, the risk potential by *A. pacificum* is higher in northern China. The number of strains available from the Yellow Sea of China is still limited, and more strains are needed for the determination of toxin profiles. It is proposed that populations between the East China Sea and Yellow Sea may be separated and may have different origins based on the distinct toxin profiles [63].

The coincidence of increased Changjiang River discharge and the resulting weakening of the China Coast Current in the summer may act as a physical barrier limiting the dispersal of *A. pacificum* cells, as also reported in larvae of the limpet *Cellana toreuma* [64]. Both of these are marine species and may not survive the freshwater plumes. Moreover, they are planktonic and rely heavily on currents for dispersal. In contrast, populations from the East and South China Sea are probably the same as there is no strong physical barrier between them. Our new strain TIO866 from the Beibu Gulf shared similar toxin profile with strains from the South China Sea, which also predominantly produce C1/2 toxins [21,24,26], thus supporting the idea of a single population. Strain TIO1210 from New Zealand produced a similar toxin profile to those from the Taiwan Strait, but differed from those in the Bay of Plenty by the lack of C3/4 [65], indicating that there are also variable strains and populations in New Zealand.

Supplementary Materials: The following are available online at <https://www.mdpi.com/article/10.3390/w13192681/s1>: Supplementary Figure S1: Gene-based calibration curves. AE, amplification efficiency. Supplementary Figure S2: Cell-based calibration curves. AE, amplification efficiency. Supplementary Figure S3: Determination of extractable gene copies per cell from the slope of the linear regression of LSU gene copies versus cell densities of *Alexandrium pacificum* based on microscopic cell counts. The mean extractable LSU copy numbers per cell was $168,550 \pm 18,780$. Supplementary Figure S4: Correlation between the number of spiked cells based on microscopic cell counts and the estimated number of cells determined by the qPCR assay. Supplementary Table S1: Sampling information of water and sediment samples in the Taiwan Strait. Supplementary Table S2: Sampling information of water samples of the three fixed stations in Xiamen Bay for qPCR. Supplementary Table S3: Sampling information of water samples of the 17 stations in Dongshan Bay for qPCR. Supplementary Table S4: DNA extraction efficiency of the NucleoSpin Soil kit. Supplementary Table S5: Toxin profiles of *Alexandrium pacificum* strains from different sea areas.

Author Contributions: Conceptualization, H.G.; methodology, M.L., J.Z., and B.K.; software, M.L.; validation, H.G.; formal analysis, M.L., J.Z., H.G. and B.K.; investigation, M.L., G.D., K.F.S., L.M. and H.G.; resources, H.G.; data curation, M.L. and J.Z.; writing—original draft preparation, M.L. and H.G.; writing—review and editing, B.K., H.G., K.F.S. and L.M.; visualization, M.L. and H.G.; supervision, H.G.; project administration, H.G.; funding acquisition, H.G. and G.D. All authors have read and agreed to the published version of the manuscript.

Funding: This project was supported by the Scientific Research Foundation of Third Institute of Oceanography, MNR (No. 2019018, 2019017) and the National Key Research and Development Program of China (No. 2019YFE0124700).

Institutional Review Board Statement: Not applicable.

Informed Consent Statement: Not applicable.

Data Availability Statement: Not applicable.

Acknowledgments: We thank two anonymous reviewers for constructive suggestions that improved the manuscript greatly.

Conflicts of Interest: The authors declare no conflict of interest.

References

1. Murray, S.A.; Ruvindy, R.; Kohli, G.S.; Anderson, D.M.; Brosnahan, M.L. Evaluation of sxtA and rDNA qPCR assays through monitoring of an inshore bloom of *Alexandrium catenella* Group 1. *Sci. Rep.* **2019**, *9*, 1–12. [[CrossRef](#)]
2. John, U.; Litaker, R.W.; Montresor, M.; Murray, S.A.; Brosnahan, M.; Anderson, D.M. Formal Revision of the *Alexandrium tamarense* Species Complex (Dinophyceae) Taxonomy: The Introduction of Five Species with Emphasis on Molecular-based (rDNA) Classification. *Protist* **2014**, *165*, 779–804. [[CrossRef](#)]
3. Hallegraeff, G.M.; Bolch, C.J.S.; Condie, S.; Dorantes-Aranda, J.J.; Murray, S.A.; Quinlan, R.; Ruvindy, R.; Turnbull, A.; Ugalde, S.; Wilson, K. Unprecedented *Alexandrium* blooms in a previously low biotoxin risk area of Tasmania, Australia. In Proceedings of the 17th International Conference on Harmful Algae, Florianopolis, Brasil, 9–14 October 2016; pp. 38–41.
4. Natsuike, M.; Yokoyama, K.; Nishitani, G.; Yamada, Y.; Yoshinaga, I.; Ishikawa, A. Germination fluctuation of toxic *Alexandrium fundyense* and *A. pacificum* cysts and the relationship with bloom occurrences in Kesenuma Bay, Japan. *Harmful Algae* **2017**, *62*, 52–59. [[CrossRef](#)] [[PubMed](#)]
5. Shin, H.H.; Li, Z.; Kim, E.S.; Park, J.-W.; Lim, W.A. Which species, *Alexandrium catenella* (Group I) or *A. pacificum* (Group IV), is really responsible for past paralytic shellfish poisoning outbreaks in Jinhae-Masan Bay, Korea? *Harmful Algae* **2017**, *68*, 31–39. [[CrossRef](#)]
6. Gu, H.; Zeng, N.; Liu, T.; Yang, W.; Müller, A.; Krock, B. Morphology, toxicity, and phylogeny of *Alexandrium* (Dinophyceae) species along the coast of China. *Harmful Algae* **2013**, *27*, 68–81. [[CrossRef](#)]
7. Gao, Y.; Yu, R.-C.; Chen, J.-H.; Zhang, Q.-C.; Kong, F.-Z.; Zhou, M.-J. Distribution of *Alexandrium fundyense* and *A. pacificum* (Dinophyceae) in the Yellow Sea and Bohai Sea. *Mar. Pollut. Bull.* **2015**, *96*, 210–219. [[CrossRef](#)] [[PubMed](#)]
8. Genovesi, B.; Laabir, M.; Masseret, E.; Collos, Y.; Vaquer, A.; Grzebyk, D. Dormancy and germination features in resting cysts of *Alexandrium tamarense* species complex (Dinophyceae) can facilitate bloom formation in a shallow lagoon (Thau, southern France). *J. Plankton Res.* **2009**, *31*, 1209–1224. [[CrossRef](#)]
9. Laabir, M.; Collos, Y.; Masseret, E.; Grzebyk, D.; Abadie, E.; Savar, V.; Sibet, M.; Amzil, Z. Influence of Environmental Factors on the Paralytic Shellfish Toxin Content and Profile of *Alexandrium catenella* (Dinophyceae) Isolated from the Mediterranean Sea. *Mar. Drugs* **2013**, *11*, 1583–1601. [[CrossRef](#)]

10. Hallegraeff, G. Transport of toxic dinoflagellates via ships' ballast water: bioeconomic risk assessment and efficacy of possible ballast water management strategies. *Mar. Ecol. Prog. Ser.* **1998**, *168*, 297–309. [[CrossRef](#)]
11. Anderson, D.M. Physiology and bloom dynamics of toxic *Alexandrium* species, with emphasis on life cycle transitions. *Nato Asi Ser. G Ecol. Sci.* **1998**, *41*, 29–48.
12. Anderson, D.M.; Keafer, B.A.; Kleindinst, J.L.; McGillicuddy, D.; Martin, J.L.; Norton, K.; Pilskaln, C.H.; Smith, J.L.; Sherwood, C.R.; Butman, B. *Alexandrium fundyense* cysts in the Gulf of Maine: Long-term time series of abundance and distribution, and linkages to past and future blooms. *Deep. Sea Res. Part II Top. Stud. Oceanogr.* **2014**, *103*, 6–26. [[CrossRef](#)]
13. Gu, H.; Lan, D.; Fang, Q.; Wang, Z.; Cai, F. Distribution and germination of *Alexandrium* sp. cysts in coastal areas of Southeast China Sea. *J. Appl. Ecol.* **2003**, *14*, 1147–1150.
14. Gu, H.F.; Fang, Q.; Li, R.X.; Lan, D.Z.; Zhu, M.Y. Preliminary study on dinoflagellate cysts in changjiang river estuary. *Oceanol. Limnol. Sin.* **2004**, *35*, 413–423.
15. Dai, L.; Geng, H.-X.; Yu, R.-C.; Liu, Y.; Zhao, J.-Y.; Wang, J.-X.; Zhang, Q.-C.; Kong, F.-Z.; Zhou, M.-J. Distribution of *Alexandrium pacificum* cysts in the area adjacent to the Changjiang River estuary, China. *Mar. Pollut. Bull.* **2020**, *156*, 111206. [[CrossRef](#)]
16. Wang, Z.; Matsuoka, K.; Qi, Y.; Chen, J.; Lü, S. Dinoflagellate cyst records in recent sediments from Daya Bay, South China Sea. *Phycol. Res.* **2004**, *52*, 396–407. [[CrossRef](#)]
17. Genovesi, B.; Mouillot, D.; Laugier, T.; Fiandrino, A.; Laabir, M.; Vaquer, A.; Grzebyk, D. Influences of sedimentation and hydrodynamics on the spatial distribution of *Alexandrium catenella/tamarensis* resting cysts in a shellfish farming lagoon impacted by toxic blooms. *Harmful Algae* **2013**, *25*, 15–25. [[CrossRef](#)]
18. Fertouna-Bellakhal, M.; Dhib, A.; Fathalli, A.; Bellakhal, M.; Chomérat, N.; Masseret, E.; Laabir, M.; Turki, S.; Aleya, L. *Alexandrium pacificum* Litaker sp. nov (Group IV): Resting cyst distribution and toxin profile of vegetative cells in Bizerte Lagoon (Tunisia, Southern Mediterranean Sea). *Harmful Algae* **2015**, *48*, 69–82. [[CrossRef](#)]
19. Jiang, T.; Xu, Y.; Li, Y.; Jiang, T.-J.; Wu, F.; Zhang, F. Seasonal dynamics of *Alexandrium tamarensis* and occurrence of paralytic shellfish poisoning toxins in bivalves in Nanji Islands, East China Sea. *Mar. Freshw. Res.* **2014**, *65*, 350. [[CrossRef](#)]
20. Zhao, S.D.; Xu, N.; Lu, S.H.; Wang, Z.H. Dynamics of *Alexandrium* population and environmental factors in Daya Bay, the South China Sea. *Ecol. Sci.* **2006**, *25*, 109–112.
21. Liu, Y.; Chen, Z.; Gao, Y.; Zou, J.; Lu, S.; Zhang, L. Identifying the Source Organisms Producing Paralytic Shellfish Toxins in a Subtropical Bay in the South China Sea. *Environ. Sci. Technol.* **2021**, *55*, 3124–3135. [[CrossRef](#)]
22. Laabir, M.; Jauzein, C.; Genovesi, B.; Masseret, E.; Grzebyk, D.; Cecchi, P.; Vaquer, A.; Perrin, Y.; Collos, Y. Influence of temperature, salinity and irradiance on the growth and cell yield of the harmful red tide dinoflagellate *Alexandrium catenella* colonizing Mediterranean waters. *J. Plankton Res.* **2011**, *33*, 1550–1563. [[CrossRef](#)]
23. Oh, S.-J.; Park, J.-A.; Kwon, H.-K.; Yang, H.-S.; Lim, W.-A. Ecophysiological Studies on the Population Dynamics of Two Toxic Dinoflagellates *Alexandrium tamarensis* and *Alexandrium catenella* Isolated from the Southern Coast of Korea—I. Effects of Temperature and Salinity on the Growth. *J. Korean Soc. Mar. Environ. Energy* **2012**, *15*, 133–141. [[CrossRef](#)]
24. Anderson, D.M.; Kulis, D.M.; Qi, Y.-Z.; Zheng, L.; Lu, S.; Lin, Y.-T. Paralytic shellfish poisoning in Southern China. *Toxicon* **1996**, *34*, 579–590. [[CrossRef](#)]
25. Wang, D.Z.; Jiang, T.J.; Hsieh, D.P. Toxin composition variations in cultures of *Alexandrium* species isolated from the coastal waters of southern China. *Harmful Algae* **2005**, *4*, 109–121. [[CrossRef](#)]
26. Wang, D.Z.; Zhang, S.G.; Gu, H.F.; Chan, L.L.; Hong, H.S. Paralytic shellfish toxin profiles and toxin variability of the genus *Alexandrium* (Dinophyceae) isolated from the Southeast China Sea. *Toxicon* **2006**, *48*, 138–151. [[CrossRef](#)]
27. Barua, A.; Ajani, P.A.; Ruvindy, R.; Farrell, H.; Zammit, A.; Brett, S.; Hill, D.; Sarowar, C.; Hoppenrath, M.; Murray, S.A. First Detection of Paralytic Shellfish Toxins from *Alexandrium pacificum* above the Regulatory Limit in Blue Mussels (*Mytilus galloprovincialis*) in New South Wales, Australia. *Microorganisms* **2020**, *8*, 905. [[CrossRef](#)]
28. Kim, C.-J.; Kim, C.-H.; Sako, Y. Paralytic shellfish poisoning toxin analysis of the genus *Alexandrium* (Dinophyceae) occurring in Korean coastal waters. *Fish. Sci.* **2005**, *71*, 1–11. [[CrossRef](#)]
29. Han, M.; Lee, H.; Anderson, D.M.; Kim, B. Paralytic shellfish toxin production by the dinoflagellate *Alexandrium pacificum* (Chinhae Bay, Korea) in axenic, nutrient-limited chemostat cultures and nutrient-enriched batch cultures. *Mar. Pollut. Bull.* **2016**, *104*, 34–43. [[CrossRef](#)] [[PubMed](#)]
30. Hadjadj, I.; Laabir, M.; Frihi, H.; Collos, Y.; Shao, Z.J.; Berrebi, P.; Abadie, E.; Amzil, Z.; Chomérat, N.; Rolland, J.L.; et al. Unsuspected intraspecific variability in the toxin production, growth and morphology of the dinoflagellate *Alexandrium pacificum* R.W. Litaker (Group IV) blooming in a South Western Mediterranean marine ecosystem, Annaba Bay (Algeria). *Toxicon* **2020**, *180*, 79–88. [[CrossRef](#)]
31. Cembella, A.D.; Sullivan, J.J.; Boyer, G.L.; Taylor, F.; Andersen, R.J. Variation in paralytic shellfish toxin composition within the *Protogonyaulax tamarensis/catenella* species complex; red tide dinoflagellates. *Biochem. Syst. Ecol.* **1987**, *15*, 171–186. [[CrossRef](#)]
32. Wang, Y.F.; Yu, R.C.; Lu, D.D.; Lü, S.H.; Zhu, D.D.; Zhang, C.S.; Yan, T.; Zhang, Q.C.; Zhou, M.J. Recurrent toxic blooms of *Alexandrium* spp. in the East China Sea-potential role of Taiwan Warm Current in bloom initiation. *J. Ecol. Toxicol.* **2018**, *2*, 115.
33. Chen, Y.Y. Assessment of quality of mariculture shellfish in the middle east of Fujian coast. *J. Fish. Res.* **2020**, *42*, 146–152.
34. Bolch, C.J.S. The use of sodium polytungstate for the separation and concentration of living dinoflagellate cysts from marine sediments. *Phycologia* **1997**, *36*, 472–478. [[CrossRef](#)]

35. Guillard, R.R.L.; Ryther, J.H. Studies of marine planktonic diatoms: I *Cyclotella nana* hustedt, and *Detonula confervacea* (cleve) Gran. *Can. J. Microbiol.* **1962**, *8*, 229–239. [CrossRef] [PubMed]
36. Liu, M.; Gu, H.; Krock, B.; Luo, Z.; Zhang, Y. Toxic dinoflagellate blooms of *Gymnodinium catenatum* and their cysts in Taiwan Strait and their relationship to global populations. *Harmful Algae* **2020**, *97*, 101868. [CrossRef]
37. Katoh, K.; Standley, D.M. MAFFT Multiple Sequence Alignment Software Version 7: Improvements in Performance and Usability. *Mol. Biol. Evol.* **2013**, *30*, 772–780. [CrossRef]
38. Hall, T. BioEdit: A User-Friendly Biological Sequence Alignment Editor and Analysis Program for Windows 95/98/NT. *Nucleic Acids Symp. Ser.* **1999**, *41*, 95–98. [CrossRef]
39. Posada, D. jModelTest: Phylogenetic Model Averaging. *Mol. Biol. Evol.* **2008**, *25*, 1253–1256. [CrossRef]
40. Ronquist, F.; Huelsenbeck, J.P. MrBayes 3: Bayesian phylogenetic inference under mixed models. *Bioinformatics* **2003**, *19*, 1572–1574. [CrossRef]
41. Stamatakis, A. RAxML-VI-HPC: Maximum likelihood-based phylogenetic analyses with thousands of taxa and mixed models. *Bioinformatics* **2006**, *22*, 2688–2690. [CrossRef] [PubMed]
42. Boc, A.; Diallo, A.B.; Makarenkov, V. T-REX: A web server for inferring, validating and visualizing phylogenetic trees and networks. *Nucleic Acids Res.* **2012**, *40*, W573–W579. [CrossRef]
43. Hariganeya, N.; Tanimoto, Y.; Yamaguchi, H.; Nishimura, T.; Tawong, W.; Sakanari, H.; Yoshimatsu, T.; Sato, S.; Preston, C.M.; Adachi, M. Quantitative PCR Method for Enumeration of Cells of Cryptic Species of the Toxic Marine Dinoflagellate *Ostreopsis* spp. in Coastal Waters of Japan. *PLoS ONE* **2013**, *8*, e57627. [CrossRef]
44. Kon, N.F.; Teng, S.T.; Hii, K.S.; Yek, L.H.; Mujahid, A.; Lim, H.C.; Lim, P.T.; Leaw, C.P. Spatial distribution of toxic *Alexandrium tamiyavanichii* (Dinophyceae) in the southeastern South China Sea-Sulu Sea: A molecular-based assessment using real-time quantitative PCR (qPCR) assay. *Harmful Algae* **2015**, *50*, 8–20. [CrossRef]
45. Zou, C.; Ye, R.-M.; Zheng, J.W.; Luo, Z.H.; Gu, H.F.; Yang, W.D.; Li, H.Y.; Liu, J.S. Molecular phylogeny and PSP toxin profile of the *Alexandrium tamarensis* species complex along the coast of China. *Mar. Pollut. Bull.* **2014**, *89*, 209–219. [CrossRef]
46. Guillard, R.R.L. Division rates. In *Handbook of Phycological Methods: Culture Methods and Growth Measurements*; Stein, J.R., Ed.; Cambridge University Press: Cambridge, UK, 1973; pp. 289–311.
47. Schlitzer, R. Ocean Data View. Available online: <http://odvw.wide> (accessed on 2 March 2021).
48. Song, X.K.; Ma, J.X.; Liu, Y.H.; Liu, L.J.; Ma, Y.Q.; Ren, L.H.; Tang, X.C. Evolution and formation of *Alexandrium tamarensis* red tide in the sea area of the Nanhuangcheng Island. *Trans. Oceanol. Limnol.* **2009**, *30*, 93–98.
49. Wu, Z.; Zhao, D.; Syvitski, J.P.; Saito, Y.; Zhou, J.; Wang, M. Anthropogenic impacts on the decreasing sediment loads of nine major rivers in China, 1954–2015. *Sci. Total. Environ.* **2020**, *739*, 139653. [CrossRef] [PubMed]
50. Townsend, D.W.; Pettigrew, N.R.; Thomas, A.C. Offshore blooms of the red tide dinoflagellate, *Alexandrium* sp., in the Gulf of Maine. *Cont. Shelf Res.* **2001**, *21*, 347–369. [CrossRef]
51. Love, R.C.; Loder, T.C.; Keafer, B.A. Nutrient conditions during *Alexandrium fundyense* blooms in the western Gulf of Maine, USA. *Deep. Sea Res. Part II Top. Stud. Oceanogr.* **2005**, *52*, 2450–2466. [CrossRef]
52. Anderson, D.M. Bloom dynamics of toxic *Alexandrium* species in the northeastern U.S. *Limnol. Oceanogr.* **1997**, *42*, 1009–1022. [CrossRef]
53. Hu, J.; Kawamura, H.; Li, C.; Hong, H.; Jiang, Y. Review on current and seawater volume transport through the Taiwan Strait. *J. Oceanogr.* **2010**, *66*, 591–610. [CrossRef]
54. Anglès, S.; Garcés, E.; Reñé, A.; Sampedro, N. Life-cycle alternations in *Alexandrium minutum* natural populations from the NW Mediterranean Sea. *Harmful Algae* **2012**, *16*, 1–11. [CrossRef]
55. Kim, Y.O.; Choi, J.; Baek, S.H.; Lee, M.; Oh, H.-M. Tracking *Alexandrium catenella* from seed-bed to bloom on the southern coast of Korea. *Harmful Algae* **2020**, *99*, 101922. [CrossRef]
56. Vila, M.; Garcés, E.; Masò, M.; Camp, J. Is the distribution of the toxic dinoflagellate *Alexandrium catenella* expanding along the NW Mediterranean coast? *Mar. Ecol. Prog. Ser.* **2001**, *222*, 73–83. [CrossRef]
57. Lilly, E.L.; Kulis, D.M.; Gentien, P.; Anderson, D.M. Paralytic shellfish poisoning toxins in France linked to a human-introduced strain of *Alexandrium catenella* from the western Pacific: Evidence from DNA and toxin analysis. *J. Plankton Res.* **2002**, *24*, 443–452. [CrossRef]
58. Genovesi, B.; Berrebi, P.; Nagai, S.; Reynaud, N.; Wang, J.; Masseret, E. Geographic structure evidenced in the toxic dinoflagellate *Alexandrium pacificum* Litaker (*A. catenella*—Group IV (Whedon & Kofoid) Balech) along Japanese and Chinese coastal waters. *Mar. Pollut. Bull.* **2015**, *98*, 95–105. [CrossRef]
59. Dai, L.; Yu, R.C.; Geng, H.X.; Zhao, Y.; Zhang, Q.C.; Kong, F.Z.; Chen, Z.F.; Zhao, J.Y.; Zhou, M.J. Resting cysts of *Alexandrium catenella* and *A. pacificum* (Dinophyceae) in the Bohai and Yellow Seas, China: Abundance, distribution and implications for toxic algal blooms. *Harmful Algae* **2020**, *93*, 101794. [CrossRef]
60. Kellmann, R.; Mihali, T.K.; Jeon, Y.J.; Pickford, R.; Pomati, F.; Neilan, B.A. Biosynthetic Intermediate Analysis and Functional Homology Reveal a Saxitoxin Gene Cluster in Cyanobacteria. *Appl. Environ. Microbiol.* **2008**, *74*, 4044–4053. [CrossRef]
61. Wang, H.; Guo, R.; Lim, W.A.; Allen, A.E.; Ki, J.S. Comparative transcriptomics of toxin synthesis genes between the non-toxin producing dinoflagellate *Cochlodinium polykrikoides* and toxigenic *Alexandrium pacificum*. *Harmful Algae* **2020**, *93*, 101777. [CrossRef] [PubMed]

62. Yoshida, T.; Sako, Y.; Uchida, A.; Kakutani, T.; Arakawa, O.; Noguchi, T.; Ishida, Y. Purification and characterization of sulfotransferase specific to O-22 of 11-hydroxy saxitoxin from the toxic dinoflagellate *Gymnodinium catenatum* (dinophyceae). *Fish. Sci.* **2002**, *68*, 634–642. [[CrossRef](#)]
63. Anderson, D.M.; Alpermann, T.J.; Cembella, A.D.; Collos, Y.; Masseret, E.; Montresor, M. The globally distributed genus *Alexandrium*: Multifaceted roles in marine ecosystems and impacts on human health. *Harmful Algae* **2012**, *14*, 10–35. [[CrossRef](#)] [[PubMed](#)]
64. Dong, Y.W.; Wang, H.S.; Han, G.D.; Ke, C.H.; Zhan, X.; Nakano, T.; Williams, G.A. The Impact of Yangtze River Discharge, Ocean Currents and Historical Events on the Biogeographic Pattern of *Cellana toreuma* along the China Coast. *PLoS ONE* **2012**, *7*, e36178. [[CrossRef](#)] [[PubMed](#)]
65. MacKenzie, L.; de Salas, M.; Adamson, J.; Beuzenberg, V. The dinoflagellate genus *Alexandrium* (Halim) in New Zealand coastal waters: Comparative morphology, toxicity and molecular genetics. *Harmful Algae* **2004**, *3*, 71–92. [[CrossRef](#)]